A Family of Buck-Type DC-DC Converters with Autotransformers

Kaiwei Yao, Yuancheng Ren, Jia Wei, Ming Xu and Fred C. Lee
Center for Power Electronics Systems
The Bradley Department of Electrical and Computer Engineering
Virginia Polytechnic Institute and State University
Blacksburg, VA 24061 USA

***Abstract*— This paper introduces a family of buck-type DC-DC converters with autotransformers, including forward, push-pull, half-bridge, and full-bridge topologies. Compared with an isolated transformer, the autotransformer has a simpler winding structure, and it only needs to transfer part of the input power, resulting in a smaller secondary winding current. Analysis shows that the autotransformer can also help to reduce the voltage stress and current ratings of power devices in the DC-DC converters. For some applications, a simple lossless passive clamp circuit can be implemented to solve the transformer leakage problems, and the gate drive is significantly improved with a simple self-adaptive dead-time-controlled bootstrap gate driver. Simulation and experimental results show that the proposed topologies are very suitable for high-frequency applications.**

Keywords-DC-DC converter; autotransformer

I. INTRODUCTION

Autotransformers are widely used in high-power AC systems when there is no galvanic isolation requirement [1~4]. Compared with an isolated transformer, which has separated primary and secondary windings, the autotransformer uses part of the primary winding as the secondary winding in a tapped version (for step-down conversion). Fig. 1 shows the difference between an isolated transformer and an autotransformer. The isolated transformer has a primary winding with n_p turns and a secondary winding with n_s turns. The autotransformer has only one winding with n_p turns. The output shares part of the winding with an $(n_p\text{-}n_s):n_s$ tapped connection.

Both transformers can transfer the same power as long as their turns ratios are the same:

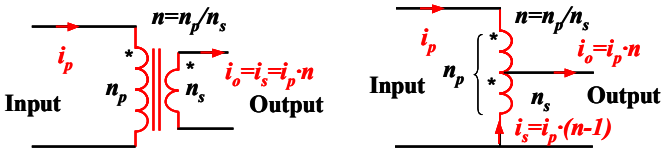

Figure 1. The comparison: (a) an isolated transformer and (b) an autotransformer.

* This work was supported by Intel, Texas Instruments, National Semiconductors, Intersil, TDK, Hitachi, Hipro, Power-One and Delta Electronics. Also, this work made use of ERC shared facilities supported by the National Science Foundation under Award Number EEC-9731677.

$$n = n_p / n_s . \quad (1)$$

But in the autotransformer, the input current goes directly to the output, reducing the secondary winding current. The secondary winding current is

$$i_s = i_p \cdot n \quad (2)$$

in the isolated transformer, and

$$i_s = i_p \cdot (n-1) \quad (3)$$

in the autotransformer. Here, i_p is the transformer primary winding current.

Furthermore, the primary winding current in the autotransformer goes through only $(n_p\text{-}n_s)$ turns winding, while in the isolated transformer, the same current goes through n_p turns winding. All of these factors mean that, for the same power transformation less copper can be used with an autotransformer as compared with an isolated transformer. The savings effect is significant, especially when the transformer turns ratio is near 1 (n>1 for step-down conversion).

The autotransformer is mostly discussed in terms of its application to the 50/60Hz high-power systems. But actually, the benefits of the autotransformer can also be extended to the high-frequency pulse width modulation (PWM) controlled DC-DC converters. A suitable application area is the voltage regulator module (VRM), which supports huge current and very low voltage to a microprocessor. Currently, the multiphase synchronous buck converter is adopted for VRMs to convert 12 V of input voltage to about 1~2 V of output voltage [5~6]. However, the small duty cycle limits its effectiveness in the high-frequency application, which is the trend for designs with high power density [7~10]. A simple method uses transformers to extend the duty cycle. Since there is no galvanic isolation requirement, buck-type converters with the autotransformer can simplify the topology and greatly improve the performance.

This paper derives a family of buck-type converters with autotransformers, which corresponds to forward, push-pull, half-bridge and full-bridge converters. For convenience, these topologies are referred to as non-isolated ones. Detailed analysis shows that these non-isolated topologies have many other advantages than those with isolation. In Section II, a non-isolated forward converter is used as an example to explain the operation principle with an autotransformer. Section III extends the concept to other topologies, with both center-tapped and current-doubler rectifiers. A prototype of a non-isolated push-

pull converter with current doubler is developed, and Section IV shows the significant performance improvement.

II. FORWARD CONVERTER WITH AN AUTOTRANSFORMER

Theoretically, all topologies with an isolated transformer can be implemented with an autotransformer. However, the autotransformer is a three-port component while the isolated transformer is a four-port component. Fig. 1 shows the difference. Normally, an isolated transformer in a topology cannot be simply replaced by an autotransformer because of the different connection. Furthermore, the autotransformer is not limited by the implementation of a tapped-winding connection, as shown in Fig. 1(b). In the DC-DC converter, the autotransformer can be implemented with two coupled windings, and switches may be put between them. This kind of flexibility offers more benefits for the DC-DC converter with autotransformers.

A forward converter is a simple example for DC-DC conversion. Fig. 2 shows the step-by-step evolution from isolated to non-isolated forward converter. A forward converter with an isolated transformer and a synchronous rectifier is shown in Fig. 2(a). For simplicity the transformer reset winding is not drawn here. The first step is to split the primary winding into two (w_{p1} and w_{p2}) so that one of the primary windings (w_{p1}) has the same number of turns as the secondary winding. The location of the primary switch Q_p is adjusted, but the series relationship with the primary winding is not changed.

In Fig. 2(b), since the primary winding w_{p1} has the same number of turns as the secondary winding, and they share a common connection point (the ground), their connection points with "*" marks can also be connected together. Then one winding is redundant and can be eliminated. Fig. 2(c) shows this modification. When Q_p and Q_s are turned on, the windings w_{p1} and w_{p2} form an autotransformer to transfer the energy.

Fig. 2(d) shows a further step of modification by equivalently moving Q_s. One benefit is the reduced conduction current through Q_s. During the turn-on period, instead of conducting the entire load current, as in Fig. 2(c), Q_s conducts the reduced secondary winding current in the autotransformer, as in Fig. 2(d). Another significant advantage is the simple gate drive for all three MOSFETs. The connection of Q_p and Q_f is a totem-pole structure, which is the same as that in a synchronous buck topology. This allows a single bootstrap gate driver to be used to drive both Q_p and Q_f [11]. Driving Q_s is also very simple because its gate signal is the same as that of Q_p and its source is connected to the ground. Fig. 3 shows the driving scheme. The bootstrap gate driver will not turn on Q_p until it senses the low-level gate signal of Q_f. Also, it will not turn on Q_f unless it senses the low-level drain-to-source voltage of Q_f. This self-adaptive control can avoid the shoot-through of Q_p and Q_f with less than 30 ns of dead time for the entire load range. For the isolated forward converter, as shown in Fig. 2(a), it is difficult to implement this type of self-adaptive drive scheme, and the fixed dead time must be designed to be large for the worst case. As a result, in the non-isolated forward converter, the body diode conduction loss of Q_f during the dead time can be reduced. The savings effect is more significant in high-frequency applications.

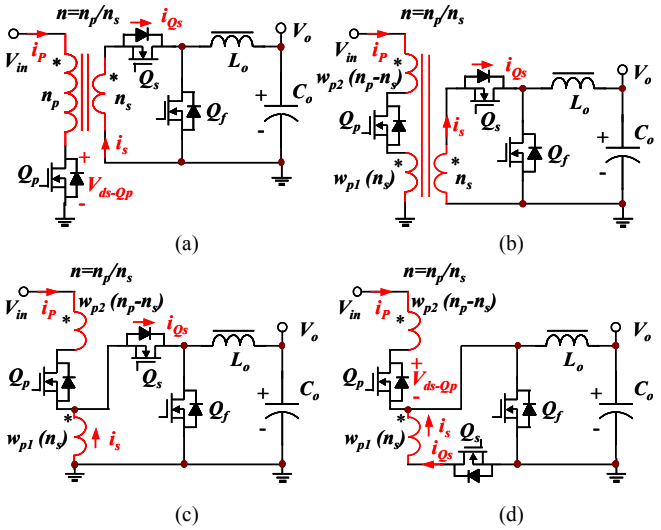

Figure 2. The evolution of the non-isolated forward converter: (a) an isolated forward converter, (b) step 1, (C) step 2 and (d) step 3.

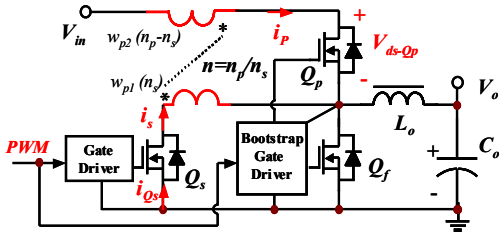

Figure 3. Gate drive for the non-isolated forward converter.

Table I shows a comparison between the isolated and non-isolated forward converters for the same power conversion in the ideal steady-state operation condition. The output load current is I_o. The inductor L_o is assumed to be large enough that the current ripple can be ignored. In Table I, the device switching currents and turn-off voltage stresses are compared. Since the duty cycles of these two topologies are the same, Table I compares only the amplitude of the transformer winding currents. It is clearly shown that the non-isolated forward converter has smaller secondary winding current i_s, smaller synchronous rectifier current i_{Qs}, and smaller Q_p turn-off voltage stress V_{ds_Qp}. The benefits are very significant when the turns ratio n is near 1. In the 12V-input VRM application, an autotransformer with a turns ratio of 2 can be used to double the duty cycle and greatly improve the efficiency.

TABLE I. COMPARISON BETWEEN THE ISOLATED AND NON-ISOLATED FORWARD CONVERTERS.

Forward Converter	Duty Cycle	Q_p		Q_s		Q_f		*Transformer*	
		i_{Qp}	V_{ds_Qp}	i_{Qs}	V_{ds_Qs}	i_{Qf}	V_{ds_Qf}	i_p	i_s
Isolated	$\frac{n \cdot V_o}{V_{in}}$	$\frac{I_o}{n}$	$2 \cdot V_{in}$	I_o	$\frac{1}{n} \cdot V_{in}$	I_o	$\frac{1}{n} \cdot V_{in}$	$\frac{I_o}{n}$	I_o
No-isolated	$\frac{n \cdot V_o}{V_{in}}$	$\frac{I_o}{n}$	$(2-\frac{1}{n}) \cdot V_{in}$	$(1-\frac{1}{n}) \cdot I_o$	$\frac{1}{n} \cdot V_{in}$	I_o	$\frac{1}{n} \cdot V_{in}$	$\frac{I_o}{n}$	$(1-\frac{1}{n}) \cdot I_o$

An active-clamped circuit can be used in the non-isolated forward converter to clamp the turn-off spike of Q_p, which occurs due to the transformer leakage inductance. Also, the

active-clamped circuit can help to reset the transformer, so that there is no need for the extra reset winding. Fig. 4(a) shows the circuit structure. The gate signal of the clamp switch Q_c is complementary to that of the main switch Q_p. Especially when the turns ratio is smaller than 2, a simple passive-clamped circuit can be used for the same purpose. Fig. 4(b) shows the circuit structure with a turns ratio n=2. C_c, D_{c1} and D_{c2} form the passive-clamped circuit. When Q_p is turned off, C_c clamps the voltage spike and stores the leakage energy. When Q_p is turned on, the extra stored energy is discharged to the output through D_{c2}. Narrow spike currents charge and discharge the clamp capacitor C_c. As a result, the clamp circuit can be very small.

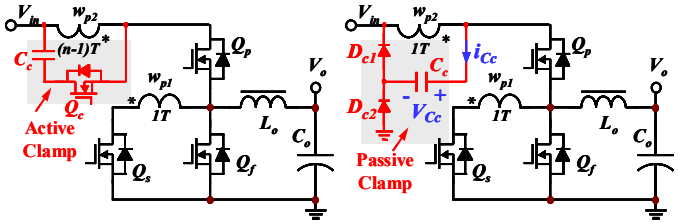

(a) (b)

Figure 4. The non-isolated forward converter: (a) with an active-clamped circuit and (b) with a passive-clamped circuit.

The simulation results in Fig. 5 show the perfect voltage-clamped effect for Q_p in a 12V-to-1.5V/15A VRM. A 30V MOSFET can still be used for Q_p to obtain a good trade-off between the switching speed and $R_{ds\text{-}on}$. According to Table I, the voltage stresses of Q_s and Q_p are much smaller, and 20V MOSFETs can be used to further reduce the conduction loss.

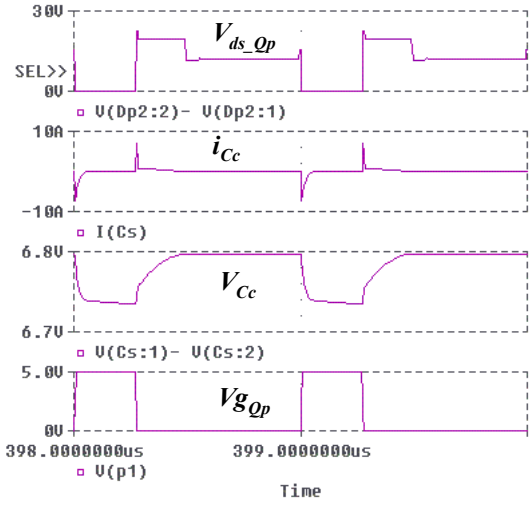

Figure 5. The effect of the passive-clamped circuit.

III. Other Converters with An Autotransformer

The idea of using autotransformers can be extended to other buck-type DC-DC converters. This section will discuss these converters one by one. In the following discussion, the turns number of the secondary winding is normalized to 1. The output load current is I_o. And the output filter inductance value is assumed to be large enough that the current ripple can be ignored.

A push-pull converter operates as two interleaved forward converters in which PWM control signals are phase-shifted by 180 degrees. There are two types of rectification circuits for this interleaving operation. One is the current-doubler rectifier with two output filter inductors. Another is the center-tapped rectifier with only one filter inductor. Both of these rectifiers can be implemented with an autotransformer. Figs. 6 and 7 show the isolated and non-isolated push-pull converters with current-doubler and center-tapped rectifiers. The gate control signals, as shown in Fig. 8, are the same for the four different versions of push-pull converters.

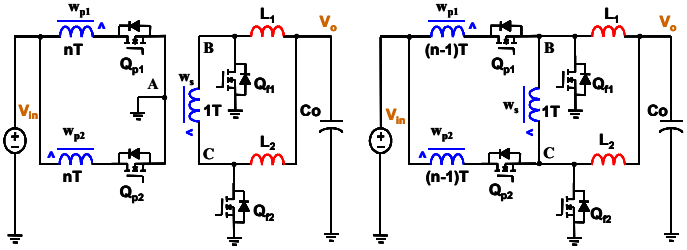

(a) (b)

Figure 6. The push-pull converter with a current-doubler rectifier: (a) with an isolated transformer and (b) with an autotransformer.

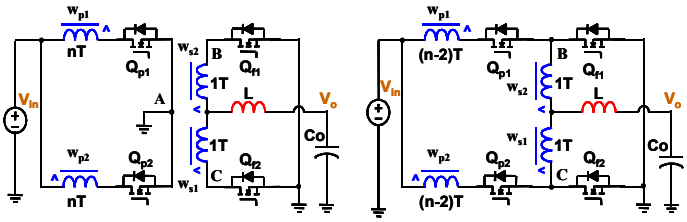

(a) (b)

Figure 7. The push-pull converter with a center-tapped rectifier: (a) with an isolated transformer and (b) with an autotransformer.

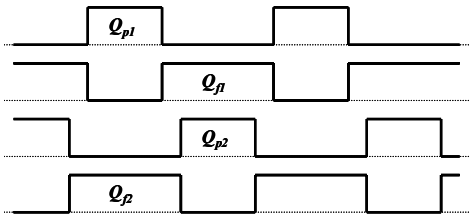

Figure 8. The gate signals for the push-pull converter.

Since the duty ratios of the primary side switches (Q_{p1} and Q_{p2}) are smaller than 50%, when Q_{p1} is on, Q_{f2} is also on. As a result, in Fig. 6(a), when Q_{p1} and Q_{f2} are on, the windings w_{p1} and w_s form an isolated transformer to transfer the energy. But in Fig. 6(b), the windings w_{p1} and w_s form an autotransformer to transfer the energy. The situation is the same when Q_{p2} and Q_{f1} are on. The only difference is that winding w_{p2} functions instead of winding w_{p1}. Because of the advantage of the autotransformer, windings w_{p1} and w_{p2} need fewer turns as compared with those in the isolated transformer.

The operation principle is similar for the non-isolated push-pull converter with a center-tapped rectifier, which is shown in Fig. 7(b). The slight difference is that the center-tapped

windings w_{s1} and w_{s2} play simultaneous roles for an autotransformer. As a result, w_{p1} and w_{p2} only require (n-2) turns to form the same turns ratio (n:1).

Both active-clamped and passive-clamped circuits can be used for the non-isolated push-pull converter to solve the problems related to the transformer leakage. The clamp circuit must be placed across windings w_{p1} and w_{p2} as shown in Fig. 4. Especially for the push-pull converter with a center-tapped rectifier, it can achieve 2:1 turns ratio without windings w_{p1}, w_{p2} or any clamp circuits. Actually, this is the same topic discussed in other work [12,13] for the inductor coupling in a two-phase synchronous buck converter. Fig. 9 shows the equality. The inductor coupling represents the effect of an autotransformer. And the leakage inductors play the same role as the output filter L. This also means that the autotransformer and the output filter inductor L can be implemented with an integrated magnetic, as discussed in [12,13].

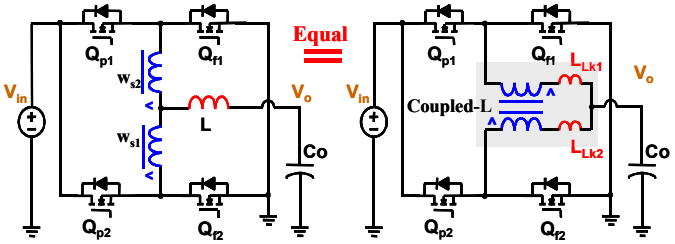

Figure 9. The equality: (a) a push-pull converter with a 2:1 autotransformer, and (b) a two-phase buck converter with inductor coupling.

The non-isolated push-pull converters can use bootstrap gate drivers, since the primary-side switches and the secondary-side switches are connected in a totem-pole structure (Q_{p1} and Q_{f1}, Q_{p2} and Q_{f2}). Also they have smaller voltage or current ratings for the power devices. Table II lists the device and winding current amplitudes as well as the device turn-off voltages. It shows an improvement similar to that of the non-isolated forward converter.

TABLE II. COMPARISON BETWEEN THE ISOLATED AND NON-ISOLATED PUSH-PULL CONVERTERS.

Push-Pull Converter		Duty Cycle (<50%)	Q_{p1}, Q_{p2}		Q_{f1}, Q_{f2}		*Transformer Current*	
			i_{Qp}	V_{ds_Qp}	i_{Qf}	V_{ds_Qf}	w_{p1}, w_{p2}	w_s / w_{s1}, w_{s2}
Center Tap	Isolated	$\frac{n \cdot V_o}{2 \cdot V_{in}}$	$\frac{I_o}{n}$	$2 \cdot V_{in}$	I_o	$\frac{2}{n} \cdot V_{in}$	$\frac{I_o}{n}$	I_o
	No-isolated	$\frac{n \cdot V_o}{2 \cdot V_{in}}$	$\frac{I_o}{n}$	$(2-\frac{2}{n}) \cdot V_{in}$	$(1-\frac{1}{n}) \cdot I_o$	$\frac{2}{n} \cdot V_{in}$	$\frac{I_o}{n}$	$(1-\frac{1}{n}) \cdot I_o$
Current Doubler	Isolated	$\frac{n \cdot V_o}{V_{in}}$	$\frac{I_o}{2 \cdot n}$	$2 \cdot V_{in}$	I_o	$\frac{1}{n} \cdot V_{in}$	$\frac{I_o}{2 \cdot n}$	$\frac{I_o}{2}$
	No-isolated	$\frac{n \cdot V_o}{V_{in}}$	$\frac{I_o}{2 \cdot n}$	$(2-\frac{1}{n}) \cdot V_{in}$	$(1-\frac{1}{2 \cdot n}) \cdot I_o$	$\frac{1}{n} \cdot V_{in}$	$\frac{I_o}{2 \cdot n}$	$(1-\frac{1}{n}) \cdot \frac{I_o}{2}$

The comparison between (a) and (b) in Figs. (7) and (8) shows the physical modification from the isolated push-pull converters to the non-isolated ones. In the isolated topologies, the ground point A is split and connected to points B and C, which cross the secondary winding. Then, the isolated transformer changes to an autotransformer. The turns of the primary windings (w_{p1} and w_{p2}) can be reduced for the same transformer turns ratio.

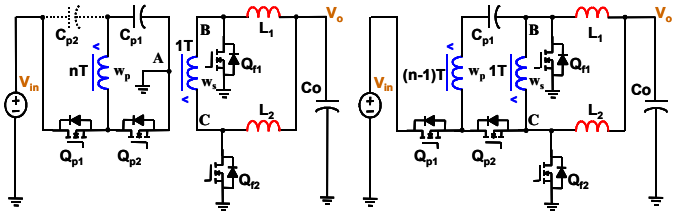

Figure 10. The half-bridge converter with a current-doubler rectifier: (a) with an isolated transformer and (b) with an autotransformer.

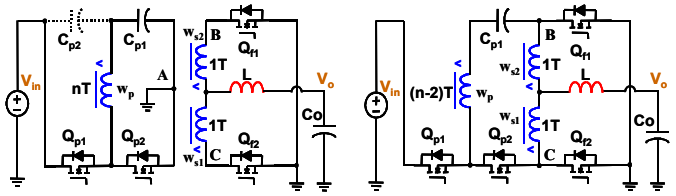

Figure 11. The half-bridge converter with a center-tapped rectifier: (a) with an isolated transformer and (b) with an autotransformer.

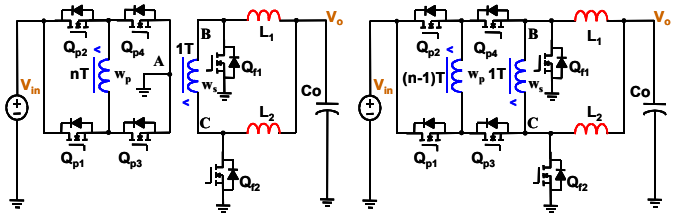

Figure 12. The full-bridge converter with a current-doubler rectifier: (a) with an isolated transformer and (b) with an autotransformer.

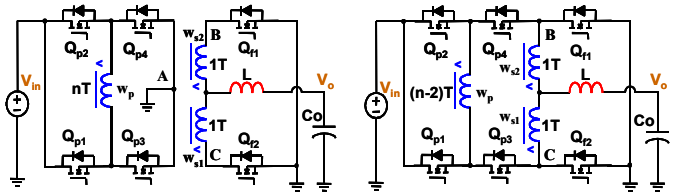

Figure 13. The full-bridge converter with a center-tapped rectifier: (a) with an isolated transformer and (b) with an autotransformer.

Following the same modification, the isolated half-bridge and full-bridge converters can be derived. Figs. 10-13 show these converters with current-doubler and center-tapped rectifiers.

For symmetrical operation of the half-bridge converters, the gate control signals are the same as those shown in Fig. 8. When Q_{p1} and Q_{f2} or Q_{p2} and Q_{f1} are on, the transformer or the autotransformer transfers the energy. In the isolated topologies, as shown in Figs. 10(a) and 11(a), the use of capacitor C_{p2} makes no difference. But in the non-isolated topologies, only one capacitor C_{p1} can be used. Adding capacitor C_{p2} in Figs. 10(b) and 11(b) will cause an AC voltage imbalance across winding w_p. Q_{p1} will be damaged by turning on a huge capacitor discharging current.

The half-bridge converters can also be controlled asymmetrically to achieve zero-voltage switching (ZVS) [14]. This paper will not discuss this operation mode, because it is no longer a buck-type converter.

For the full-bridge converters, both phase-shifted and PWM control methods can be used. When Q_{p1}, Q_{p4} and Q_{f2} or Q_{p2}, Q_{p3} and Q_{f1} are on, the transformer or the autotransformer transfers the energy. During all other periods, the currents are freewheeling. More detailed analysis has been done in [15] for the non-isolated full-bridge converter with a current-doubler rectifier. The operation principle of using a center-tapped rectifier is the same, except that the tapped windings w_{s1} and w_{s2} play simultaneous roles for an autotransformer.

The gate driving for the non-isolated half-bridge and full-bridge converters is a little more complicated. As shown in Figs. 10(b) and 11(b), a bootstrap gate driver can still be used to drive $Q_{p2}$and Q_{f2}. But driving $Q_{p1}$and Q_{f1} is different, since they are no longer in a totem-pole structure. For the non-isolated full-bridge converters, each of the primary switches ($Q_{p1\sim p4}$) needs a bootstrap driver.

There is no need for a clamp circuit in the non-isolated half-bridge and full-bridge converters because of their bridge structures. For example, in Fig. 10(b), when Q_{p1} is turned off, the body diode of Q_{p2} supports a path for the leakage current. As a result, the turn-off voltage stress of Q_{p1} is clamped to the input voltage V_{in}. This is a significant benefit for the bridge-type converters.

Tables III and IV show the current or voltage rating reduction effect for the non-isolated bridge-type converters. The device and winding current amplitudes and the device voltage stresses are compared.

The non-isolated half-bridge converter is very promising in extending the duty cycle. For example, in Fig. 10(b), two single-turn coupled windings can extend the duty cycle by 4 times compared with that in the buck converter.

TABLE III. COMPARISON BETWEEN THE ISOLATED AND NON-ISOLATED HALF-BRIDGE CONVERTERS

Half-Bridge Converter		Duty Cycle (<50%)	Q_{p1}, Q_{p2}		Q_{f1}, Q_{f2}		*Transformer Current*	
			i_{Qp}	V_{ds_Qp}	i_{Qf}	V_{ds_Qf}	w_{p1}, w_{p2}	w_s / w_{s1},w_{s2}
Center Tap	Isolated	$\frac{n\cdot V_o}{V_{in}}$	$\frac{I_o}{n}$	V_{in}	I_o	$\frac{V_{in}}{n}$	$\frac{I_o}{n}$	I_o
	No-isolated	$\frac{n\cdot V_o}{V_{in}}$	$\frac{I_o}{n}$	$(1-\frac{1}{n})\cdot V_{in}$, V_{in}	$(1-\frac{1}{n})\cdot I_o$	$\frac{V_{in}}{n}$	$\frac{I_o}{n}$	$(1-\frac{1}{n})\cdot I_o$
Current Doubler	Isolated	$\frac{2\cdot n\cdot V_o}{V_{in}}$	$\frac{I_o}{2\cdot n}$	V_{in}	I_o	$\frac{V_{in}}{2\cdot n}$	$\frac{I_o}{2\cdot n}$	$\frac{I_o}{2}$
	No-isolated	$\frac{2\cdot n\cdot V_o}{V_{in}}$	$\frac{I_o}{2\cdot n}$	$(1-\frac{1}{2\cdot n})\cdot V_{in}$, V_{in}	$(1-\frac{1}{2\cdot n})\cdot I_o$	$\frac{V_{in}}{2\cdot n}$	$\frac{I_o}{2\cdot n}$	$(1-\frac{1}{n})\cdot\frac{I_o}{2}$

TABLE IV. COMPARISON BETWEEN THE ISOLATED AND NON-ISOLATED FULL-BRIDGE CONVERTERS

Full-Bridge With Phase-Shift Control		Duty Cycle (<50%)	Q_{p1}, Q_{p2}, Q_{p3}, Q_{p4}		Q_{f1}, Q_{f2}		*Transformer Current*	
			i_{Qp}	V_{ds_Qp}	i_{Qf}	V_{ds_Qf}	w_{p1}, w_{p2}	w_s / w_{s1},w_{s2}
Center Tap	Isolated	$\frac{n\cdot V_o}{2\cdot V_{in}}$	$\frac{I_o}{n}$	V_{in}	I_o	$\frac{2\cdot V_{in}}{n}$	$\frac{I_o}{n}$	I_o
	No-isolated	$\frac{n\cdot V_o}{2\cdot V_{in}}$	$\frac{I_o}{n}$	V_{in}	$(1-\frac{1}{n})\cdot I_o$	$\frac{2\cdot V_{in}}{n}$	$\frac{I_o}{n}$	$(1-\frac{1}{n})\cdot I_o$
Current Doubler	Isolated	$\frac{n\cdot V_o}{V_{in}}$	$\frac{I_o}{2\cdot n}$	V_{in}	I_o	$\frac{V_{in}}{n}$	$\frac{I_o}{2\cdot n}$	$\frac{I_o}{2}$
	No-isolated	$\frac{n\cdot V_o}{V_{in}}$	$\frac{I_o}{2\cdot n}$	V_{in}	$(1-\frac{1}{2\cdot n})\cdot I_o$	$\frac{V_{in}}{n}$	$\frac{I_o}{2\cdot n}$	$(1-\frac{1}{n})\cdot\frac{I_o}{2}$

Tables I~IV show that the autotransformer can help to reduce the current stress through the secondary winding and the synchronous rectifiers. It can also help to reduce the voltage stress of the primary-side switches. One exception is the non-isolated full-bridge converter, in which the voltage stress of the primary-side switches does not change. But since it can achieve ZVS, there is no penalty. For the 12V-input VRM applications, compared with a conventional multiphase buck converter, an autotransformer can use a simple winding structure to easily extend the duty cycle. The 30V trench MOSFETs can still be used for the primary-side switches to achieve fast switching speed. And the lower voltage stress of the synchronous rectifiers (the switches in the secondary side) allows the use of MOSFETs with smaller R_{ds_on}. As a result, the non-isolated topologies are expected to achieve higher efficiency than the conventional multiphase synchronous buck converter with only a slight increase of the circuit complexity.

IV. EXPERIMENTAL RESULTS

Some work has already been done to demonstrate the improvement by using an autotransformer. The two-phase buck converter with inductor coupling [12] actually represents a non-isolated push-pull converter with a 2:1 transformer turns ratio. The efficiency is improved by 2% at the full load for a 5V-to-2V/30A VRM at a switching frequency of 300 KHz.

The phase-shifted buck [15] is the case of an isolated full-bridge converter with a current-doubler rectifier. Two single-turn windings form an autotransformer, which doubles the duty cycle. Compared with the conventional two-phase buck converter, the new approach improves the full load efficiency by 6% for a 12V-to-1.5V/25A VRM at a switching frequency of 1 MHz.

CPES has developed another prototype for a 12V-to-1.5V/25A VRM based on the non-isolated push-pull converter with a current-doubler rectifier because of its simple winding structure, small winding current, and simple gate drive. Compared with a two-phase buck converter, the proposed one only needs to add an autotransformer and the related clamp circuits. It can use the same power components, gate drivers and controller. Fig. 14 shows the detailed circuit structure.

To make a comparison, a two-phase buck converter is also developed with the same power devices and output filter design. Since the output inductor values are the same, these two VRMs can achieve the same transient response with the same control bandwidth design [16, 17].

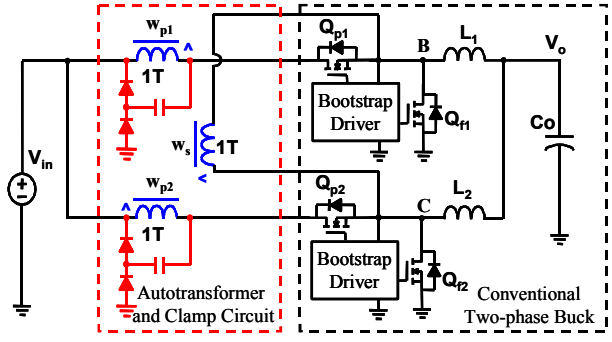

Figure 14. The non-isolated push-pull converter with a current doubler.

The operation switching frequency is set to 1 MHz in order to reduce the passive component size. A TDK EIR-18 planar core is used for the autotransformer. Nine-layer, two-ounce PCB with a fully interleaved structure is used for the three windings. Five layers in parallel are used for w_s, and two layers in parallel for w_{p1} and w_{p2}. The output filter uses two surface-mounted inductors (FP4-200nH from Cooper Electronic Technology) and four surface-mounted ceramic capacitors (100µF/6.3V from TDK).

For the power stage, Hitachi's 30V trench MOSFETs with SO-8 lead-free packaging are used for their small parasitics and excellent thermal performance. HAT2116H is used for the primary-side switches Q_{p1} and Q_{p2} because of its fast switching speed. HAT2099H is used for the synchronous rectifiers Q_{f1} and Q_{f2} as a trade-off between conduction and driving losses. The gate driver is National Semiconductor's LM2726, which has fast driving capability and can drive both the top and bottom switches. It uses the self-adaptive control scheme to limit the dead times to about 25 ns, so there is no shoot-through problem and the body-diode conduction loss is small.

For the clamp circuit, two 1A/25V Schottky diodes and one 4.7µF ceramic capacitor are used. Their sizes are very small. Fig. 15(a) shows that the voltage stress across the primary side switch Q_{p1} is perfectly clamped to 20 V. The transformer leakage energy can be stored in the clamp capacitor and then recovered to the output. Furthermore, the synchronous rectifier voltage stress waveform V_{ds_f1} shows that the clamp circuit can also reduce the voltage ringing when the top switch is turned on. This can help to attenuate the body diode reverse-recovery loss.

Fig. 15 shows the operation waveform comparison between the proposed topology and the two-phase buck converter at 1 MHz. The proposed topology doubles the duty cycle and halves the voltage stress of the synchronous rectifiers. All of these indicators predict a significant reduction of losses related to switching frequency. Fig. 16 shows the power stage efficiency improvement at 1 MHz of switching frequency. Compared with the conventional two-phase buck converter, the new approach improves the full load efficiency by 6%. And Fig. 17 shows the developed prototype. With all surface mounted components, the power density is around 70W/in^3.

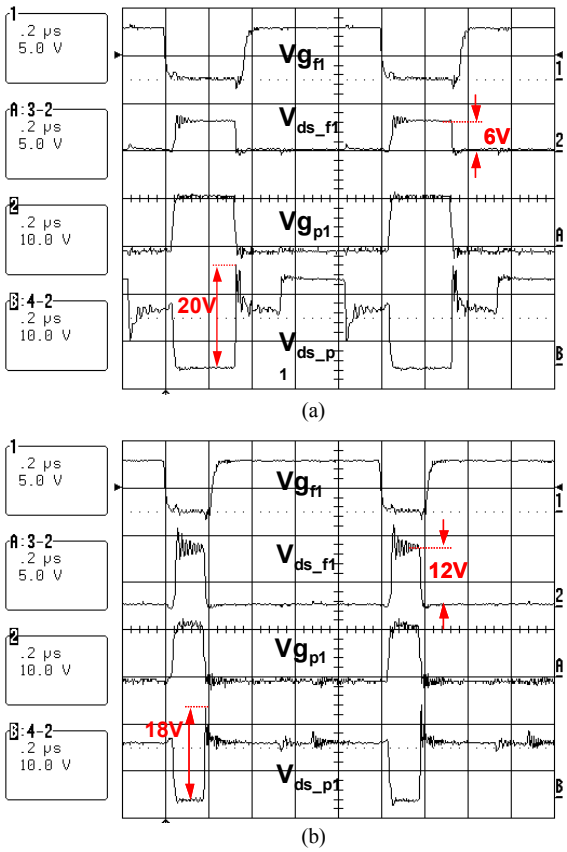

Figure 15. The comparsion of the operation waveforms at 1 MHz: (a) the non-isolated push-pull converter and (b) the two-phase buck converter.

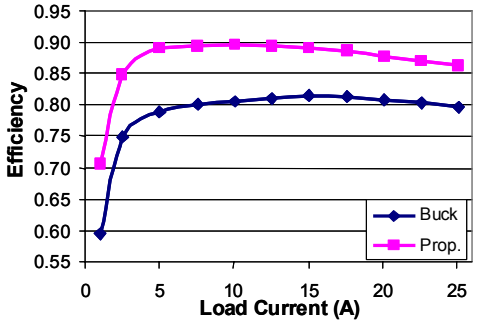

Figure 16. The efficiency comparsion.

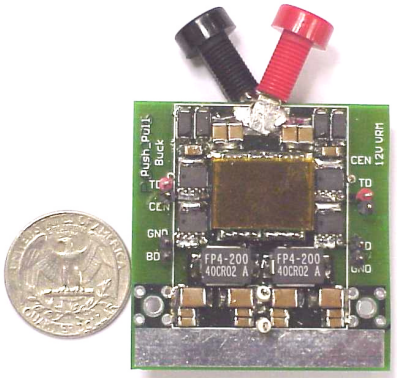

Figure 17. The prototype for the non-isolated push-pull converter.

V. Conclusion

This paper introduces a family of buck-type DC-DC converters implemented with autotransformers. The advantages are discussed in detail. The analysis shows that these topologies are especially suitable for the 12V-input VRM application. Experimental results show the significant efficiency improvement compared with the conventional multiphase buck converter.

Acknowledgments

The authors would like to thank Hitachi, TDK, National Semiconductor and Cooper Electronic Technology for supplying free samples.

REFERENCES

[1] W. Kellerman, H.M. El-Din, C.E. Graham and G.A. Maria, "Optimization of fixed tap transformer setting in bulk electric systems," in *IEEE Trans. Power Systems*, vol. 6, pp. 1126–1132, Aug. 1991.

[2] J.P.G. Abreu, C.A.M. Guimaraes and G. Paulillo, "A proposal for a power converter autotransformer," in *Proc. IEEE Electric Machines and Drives*, 1997, pp. TC3/6.1–TC3/6.4.

[3] M. Kang, B.O. Woo, P.N. Enjeti and I.J. Pitel, "Auto-connected electronic transformer (ACET) based multi-pulse rectifiers for utility interface of power electronic systems," in *Proc. IEEE IAS*, 1998, pp. 1554–1561.

[4] R.G. Andrei, M.E. Rahman, C. Koeppel and J.P. Arthaud, "A novel autotransformer design improving power system operation," in *IEEE Trans. Power Delivery*, vol. 17, pp. 523–527, April 2002.

[5] X. Zhou, X. Zhang, J. Liu, P. Wong, J. Chen, H. Wu, L. Amoroso, F. C. Lee and D. Y. Chen, "Investigation of candidate VRM topology for future microprocessors," in *Proc. IEEE APEC*, 1998, pp. 145–150.

[6] "Multiphase controller meets Pentium's power demands," *EDN*, p. 28, Aug. 3, 1998.

[7] P. Xu, J. Wei and F.C. Lee, "The active-clamp couple-buck converter-a novel high efficiency voltage regulator module," in *Proc. IEEE APEC*, 2001, pp. 252–257.

[8] P. Xu, J. Wei, K. Yao, Y. Meng and F.C. Lee, "Investigation of candidate topologies for 12V VRM," in *Proc. IEEE APEC*, 2002, pp. 686–692.

[9] K. Yao, Y. Meng and F.C. Lee, "A novel winding coupled buck converter for high step-down DC/DC conversion," in *Proc. IEEE PESC*, 2002, pp. 651–656.

[10] "LM2725/LM2726 high speed synchronous MOSFET drivers," in *data sheet of National Semiconductor*, Nov. 2000.

[11] P. Wong, P. Xu, B. Yang and F.C. Lee, "Performance improvements of interleaving VRMs with coupling inductors," in *IEEE Trans. Power Electro.*, vol. 16, July 2001, pp. 499–507.

[12] J. Li, C.R. Sullivan and A. Schultz, "Coupled-inductor design optimization for fast-response low-voltage DC-DC converters," in *Proc. IEEE APEC*, 2002, pp. 817–823.

[13] T. Ninomiya, N. Matsumoto, M. Nakahara and K. Harada, "Static and dynamic analysis of zero-voltage-switched half-bridge converter with PWM control," In *Proc. IEEE PESC*, 1991, pp. 230–237.

[14] J. Wei and F.C. Lee, "A novel soft-switched high-frequency high-efficiency high-current 12V voltage regulator," in *Proc. IEEE APEC*, 2003.

[15] P.L. Wong, F.C. Lee, P. Xu and K. Yao, "Critical inductance in voltage regulator modules," in *Proc. IEEE APEC*, 2002, pp. 203–209.

[16] K. Yao, Y. Meng and F.C. Lee, "Control bandwidth and transient response of buck converters," in *Proc. IEEE PESC*, 2002, pp. 137–142.